Diversification and introgression in four chromosomal taxa of the Pearson's horseshoe bat (*Rhinolophus pearsoni*) group

Weiwei Zhou[1], Neil M. Furey[2], Pipat Soisook[3], Vu D. Thong[4,5], Burton K. Lim[6], Stephen J. Rossiter[7*], Xiuguang Mao[1*]

1 *School of Ecological and Environmental Sciences, East China Normal University, Shanghai 200062, China*

2 *Fauna & Flora International (Cambodia), PO Box 1380, No. 19, Street 360, Boeng Keng Kong 1, Phnom Penh, 12000, Cambodia*

3 Princess Maha Chakri Sirindhorn Natural History Museum, Prince of Songkla University, Hat Yai, Songkhla 90110, Thailand

4 Institute of Ecology and Biological Resources, Vietnam Academy of Science and Technology (VAST), 18 Hoang Quoc Viet Road, Cau Giay District, Hanoi, Vietnam

5 Graduate University of Science and Technology, VAST, Vietnam

6 Department of Natural History, Royal Ontario Museum, Toronto, Ontario M5S 2C6, Canada

7 School of Biological and Behavioural Sciences, Queen Mary University of London, London E1 4NS, UK

*Corresponding author: xgmao@sklec.ecnu.edu.cn; s.j.rossiter@qmul.ac.uk;

Running title: Introgression among chromosomal taxa of bats

Abstract

Chromosomal variation among closely related taxa is common in both plants and animals, and can reduce rates of introgression as well as promote reproductive isolation and speciation. In mammals, studies relating introgression to chromosomal variation have tended to focus on a few model systems and typically characterized levels of introgression using small numbers of loci. Here we took a genome-wide approach to examine how introgression rates vary among four closely related horseshoe bats (*Rhinolophus pearsoni* group) that possess different diploid chromosome numbers (2n=42, 44, 46, and 60) resulting from Robertsonian (Rb) changes (fissions/fusions). Using a sequence capture we obtained orthologous loci for thousands of nuclear loci, as well as mitogenomes, and performed phylogenetic and population genetic analyses. We found that the taxon with 2n = 60 was the first to diverge in this group, and that the relationships among the three other taxa (2n=42, 44 and 46) showed discordance across our different analyses. Our results revealed signatures of multiple ancient introgression events between the four taxa, with evidence of mitonuclar discordance in phylogenetic trees and reticulation events in their evolutionary history. Despite this, we found no evidence of recent and/or ongoing introgression between taxa. Overall, our results indicate that the effects of Rb changes on the reduction of introgression are complicated and that these may contribute to reproductive isolation and speciation in concert with other factors (e.g. phenotypic and genic divergence).

Keywords: chromosomal rearrangements, target capture, hybridization, reproductive isolation, bats

1. Introduction

Chromosomal variation, including changes in diploid number (2n) of chromosomes as well as structural rearrangements (fissions/fusions, translocations, and inversions), are widely reported in plants and animals. By interfering with normal meiosis, chromosomal differences can reduce heterozygote fitness (White, 1978; King, 1995), potentially driving reproductive isolation and speciation (Dobzhansky, 1971; King, 1995; Rieseberg, 2001; Faria & Navarro, 2010; Lucek et al., 2022), with cases of chromosomal speciation described in diverse taxa (Navarro & Barton, 2003; Rieseberg & Livingstone, 2003; Ayala & Coluzzi, 2005; Charron et al., 2014).

Two common forms of chromosomal rearrangement that appear to be particularly important in promoting reproductive isolation are Robertsonian (Rb) fusions and fissions. Indeed, Rb rearrangements have been linked to restricted introgression between chromosomal taxa (race or species) (e.g. Cicconardi et al., 2021; de Vos et al., 2020; Potter et al., 2022), although exceptions occur (Searle, 1993; Searle, Polly, & Zima, 2019; King, 1995; Giménez et al., 2017). Chromosomal fusions, like chromosomal inversions, have also been reported to contribute to adaptation (e.g. Wellband et al., 2019; Liu et al., 2022). In addition, Rb fusions/fissions can even promote homoploid hybrid speciation by fixation of novel Rb fusions/fissions in hybrid taxon that originate from hybridization of different chromosomal taxa (e.g. Lukhtanov et al., 2015; Leducq et al., 2016). Yet despite these findings, few studies examining the role of Rb fusions/fissions in divergence and speciation have been conducted using genome-wide data (but see Potter et al., 2022; Franchini et al., 2020; Cicconardi et al., 2021). These few previous studies suggest that Rb fusions may have little effects on the fertility of hybrids and thus may play a minor role in causing reproductive isolation. To generate a consensus conclusion about the role of Rb changes in the reduction of introgression, more studies in other organism systems are needed.

Bats (order Chiroptera) are the second largest mammalian order with over 1400 species (Simmons & Cirranello, 2020) (https://www.batnames.org/). Although there have been relatively few studies of the role of chromosomal variation in diversification of bats at a genome scale, they appear to show extensive chromosome diversity with 2n ranging from 14 to 62 (Sotero-Caio et al., 2017). Here, differences in chromosome number across taxa appear to have been mainly caused by chromosomal fusions and fissions, as also reported in other organisms, including lepidopterans (de Vos et al., 2020), rock-wallabies (Potter et al., 2017) and shrews (Searle et al., 2019). Previous karyotypic analyses using fluorescence in situ hybridization and G-banding have also revealed that Rb rearrangements are the most common types of chromosomal changes (Ao et al., 2007; Mao et al., 2008; Sotero-Caio et al., 2017), in particular in horseshoe bats (*Rhinolophus*) (Mao et al., 2007). The *Rhinolophus* genus contains over 100 recognized species, which appear to have diversified rapidly (Hutson et al., 2019). Interestingly, although most species possess 2n of either 58 or 62 chromosomes, some clades show extensive karyotypic diversity (2n = 28 to 62) (Zima et al., 1992; Sotero-Caio et al., 2017). For example, different chromosome numbers have been reported to occur among members of the *R. hipposideros* group (2n=54, 56 and 58), *R. rouxi* group (2n=36 and 56) and the *R. pearsoni* group (Sotero-Caio et al., 2017), the latter two of which are closely related and both belong to Asian clade (Sotero-Caio et al., 2017). Thus, *Rhinolophus* appears to be a promising genus in which to investigate the role of Rb fusions and fissions in divergence and speciation.

Here, we take a genome-wide approach to assess diversification and introgression in closely related, but chromosomally distinct members of the *R. pearsoni* group. This clade includes four species that have been described based on morphological and cytogenetic (chromosome) differences: *R. pearsoni*, *R. yunanensis*, *R. chiewkweeae*, and *R. thailandensis* (Hutson et al., 2019; Yoshiyuki & Lim, 2005; Wu et al., 2009). Four chromosomal taxa have been documented to date, although *R. chiewkweeae* has not yet been examined. Specifically, *R. p. chinensis*, *R. p. pearsoni*, *R. yunanensis*,

and *R. thailandensis* are characterised by 2n of 42, 44, 46 and 60, respectively (Table 1 and Figure 1a). Such reported karyotypes are based on multiple individuals, including two of *R. p. pearsoni* (Mao et al., 2007) and five of *R. yunanensis* (Wu et al., 2009), both of which were studied with G-banding. Other species' chromosomal numbers have been inferred from conventional karyotyping approaches, including *R. p. chinensis* (n=5, Zhang, 1985) and *R. thailandensis* (n=2, Harada et al., 1985; n=1 Wu et al., 2009). To date, more informative molecular cytogenetic methods (e.g. chromosome painting) have only been applied to *R. p. pearsoni* (Mao et al., 2007), and thus it is difficult to assess whether additional chromosomal rearrangements (e.g. inversions) have occurred across these four chromosomal taxa. In addition, as far as we know, no chromosomal polymorphisms have been described in each species of the *pearsoni* group.

Within our study group, *R. pearsoni* is the only one to include two recognized subspecies (*R. p. chinensis* and *R. p. pearsoni*). The subspecies of *R. p. chinensis* is restricted to eastern China while *R. p. pearsoni* occurs across South Asia, China, and Southeast Asia (Hutson et al., 2019; Bates et al., 2019). *Rhinolophus yunanensis* also has a wide distribution across China, India, Myanmar and Thailand (Hutson et al., 2019; Wu et al., 2009; Bates et al., 2019). In contrast, *R. chiewkweeae* and *R. thailandensis* were regarded as endemic species to Malaysia (Yoshiyuki & Lim, 2005; Morni et al., 2016; Waldien, 2020) and northern Thailand (Wu et al., 2009; Bouillard, 2021), respectively. We previously reported evidence of introgression of mitochondrial and nuclear DNA between *R. p. chinensis* and *R. p. pearsoni* in their contact region (Figure 1a, Mao et al., 2010, 2016), although the small number of loci examined precluded quantification of the extent of this gene flow. In addition, little is currently known about the levels of divergence and introgression among all four chromosomal taxa in the *pearsoni* group.

To study the role of chromosomal changes in introgression and diversification, it is important to first

reconstruct the evolutionary history of closely related taxa that show chromosomal variation (e.g. Franchini et al., 2020; Potter et al., 2022). In this study, we aim to relate introgression to chromosome numbers across members of the *pearsoni* group. To this end, we first generated a *de novo* assembly of a draft genome for *R. p. chinensis*. We then collected representative individuals from all four chromosomal taxa, and screened these at over 1,500 loci using a sequence capture approach. Using phylogenetic and population genetic analyses, our first aim was to clarify the currently recognized taxa in the *pearsoni* group and reconstruct their phylogenetic relationships. Second, we tested for signatures of ancient and/or recent introgression between the four chromosome taxa. Specifically, we test the hypotheses, as suggested in few previous studies with genome-wide data (Cicconardi et al., 2021; Potter et al., 2022; Franchini et al., 2020) that Rb changes may have little effects on the reduction of introgression and they contribute to reproductive isolation together with other factors (e.g. phenotypic differences).

2. Materials and methods

2.1 Sampling

To reconstruct phylogenetic relationships among taxa of the *pearsoni* group, we sampled 82 individuals from 32 localities across the known distributions of all four currently recognized chromosomal taxa, including 14 *R. p. chinensis*, 55 *R. p. pearsoni*, 4 *R. yunanensis*, and 9 *R. thailandensis* (Figure 1a and Supp. Table S1). Among these, 24 were from specimens that were assigned to taxa based on morphology by the original field collectors or museums, and were later retrospectively reclassified based on our current results (Supp. Table S1). One individual of *Hipposideros armiger* was included as an outgroup. For 24 individuals, muscle tissues were collected from the vouchers deposited in the museums (Supp. Table S1). For the remaining individuals, we took 3-mm wing membrane biopsies using a dermatological punch, releasing bats at their sites of capture. Tissue samples were stored in 95% ethanol at -20°C until DNA extraction. Genomic DNA was extracted with DNeasy kits (Qiagen) and quantified using a Qubit 2.0 Fluorimeter.

2.2 Assembly of a draft genome

For SNPs calling, we first sequenced and *de novo* assembled a draft genome for *R. p. chinensis.* A single female bat was euthanized, from which we collected fresh tissues (muscle, liver, brain, and kidney) for flash freezing in liquid nitrogen and subsequent storage at -80 °C. Sampling and tissue collection procedures were approved by the National Animal Research Authority, East China Normal University (approval ID Rh20200801).

We extracted high molecular weight DNA from muscle tissue and constructed four DNA libraries: one based on 500 bp inserts and three mate-pair libraries based on 2,000 bp, 5,000 bp and 10,000 bp inserts. Libraries were constructed and sequenced on an Illumina HiSeq 4000 sequencing platform (150 bp pair-end) at Novogene (Beijing, China). Raw sequencing reads were assessed using FastQC

version 0.11.8 (Andrews, 2010) and processed using Trimmomatic version 0.38 (Bolger et al., 2014) to remove adapter sequences and low quality bases with the parameters of SLIDINGWINDOW:4:20. We assembled sequence data using SOAPdenovo 2.04 (Luo et al., 2012) with a k-mer value of 61. Scaffolds of <1000 bp were removed from the final assembly. The completeness of the draft genome was assessed using BUSCO version 5.3.0 (Simão et al., 2015). Raw reads generated from genome sequencing have been deposited to the NCBI Sequence Read Archive (SRA) under Bioproject PRJNA906200.

2.3 Targeted gene resequencing and data analysis

For each individual, we generated sequences of 1,692 nuclear protein-coding genes and 13 mitochondrial protein-coding (MPC) genes using a targeted capture strategy. Genomic DNA library construction, hybridization between baits and libraries, and recovery of baited libraries, have been described previously (Bailey et al., 2016; Mao et al., 2019, 2020). We sequenced 83 DNA libraries using a Hiseq2500 (Illumina, 150 bp paired-end). Raw reads generated in targeted gene resequencing have been deposited to the NCBI Sequence Read Archive (SRA) under Bioproject PRJNA906200.

Raw sequencing reads were assessed using FastQC version 0.11.8 (Andrews, 2010) and trimmed using Trimmomatic v.0.38 (Bolger et al., 2014) with the parameters of SLIDINGWINDOW:4:20. Reads with the length <50 bp were discarded. Then, we generated two different datasets including sequence alignments and SNPs. Sequence alignments of nuclear exons and MPC genes were generated using SECAPR pipeline v. 2.1.0 (Andermann et al., 2018). Briefly, trimmed reads were assembled *de novo* into contigs using SPAdes 3.13.1 (Bankevich et al., 2012). Then, we extracted targeted contigs using BLASTZ (Schwartz et al., 2003) with find_target_contigs module in SECAPR. We used the same reference sequences as in Mao et al. (2019, 2020), including sequences of a total of 12,227 nuclear exons and 13 MPC genes. After removing potential paralogous loci identified with the find_target_contigs module, an average of 8544 exon sequences across all

individuals were retained, ranging from 4,242 to 10,714 (Supp. Table S2). We also obtained 13 MPC genes for all individuals and each gene was aligned using MAFFT v7.490 (Katoh et al., 2002) with default settings. To reduce the effect of missing individuals on the phylogenetic analysis, we only kept the sequence alignments sampled in > 66 individuals (i.e. > 80 % of all individuals used in this study). The remaining sequence alignments were further trimmed using trimAI v1.4 (Capella-Gutiérrez et al., 2009) with default settings except for -gt of 0.8. A final of 6458 exon alignments with the length of > 250 bp and 13 MPC gene alignments were retained for the downstream analyses. For species tree inference using ASTRAL (see below), we only used exon alignments with the length of ≥ 500 bp and with the inclusion of the outgroup, resulting in 1153 exon alignments.

To call SNPs, clean reads of each individual were mapped onto the draft genome assembly of *R. p. chinensis* using BWA-MEM Version 0.7.17 (Li & Durbin, 2010) with default settings. SAMtools Version 1.7 (Li et al., 2009) was used to generate sorted BAM files and remove potential PCR duplicates. We used BCFtools Version 1.7 (Li et al., 2011) to call SNPs for all 82 ingroup samples, which was repeated with the outgroup included. To generate high quality SNPs, we kept the biallelic SNPs with the minimum mapping quality of 30, minimum base quality of 30 and 10 < read depth < 250 for each individual. We also filtered out sites with missing data in any individuals and minor allele frequency less than 0.05. Then, BAYESCAN v2.1 (Foll & Gaggiotti, 2008) was used to detect loci under selection with the default settings. We identified 128 SNPs that showed evidence of selection with 95% of the posterior distribution of alpha significantly different from zero ($p < 0.05$ adjusted for the false discovery rate, Supp. Figure S1). After removing these outlier loci, a final of 16,164 and 4,339 SNPs were retained for all ingroup individuals and for all individuals including the outgroup, respectively. Relatedness among individuals were assessed using VCFtools v0.1.16 (Danecek et al., 2011) with the --relatedness2 parameter (Manichaikul et al., 2010) and no samples were found to be highly related (see detailed kinship coefficients in Supp. Table S3). We further used

VCFtools to filter out SNPs with possible linkage disequilibrium (--thin 10-kb), resulting in 2838 unlinked SNPs based on the 82 ingroup individuals, and 1590 SNPs when the outgroup was included.

2.4 Phylogenetic analysis on ncDNA

Exon alignments (n = 6458; total 1,977,201 bp) were concatenated and used for maximum-likelihood (ML) tree construction in IQ-TREE v1.6.12 (Nguyen et al., 2015) with the best-fit model estimated using ModelFinder (Kalyaanamoorthy et al., 2017). Node support values were estimated with 1,000 ultrafast bootstraps (Hoang et al., 2018). To account for incomplete lineage sorting (ILS), we also used a coalescent-based method to infer a species tree using ASTRAL-III version 5.7.1 (Zhang et al., 2018) with default settings. This analysis was based on multispecies coalescent (MSC) model and required individual gene trees as the input. IQ-TREE was used to infer the best ML tree for each exon alignment (1153 exon alignments, each >=500 bp) with the same procedure as the above.

To complement to phylogenetic analysis based on sequence alignments, we also inferred phylogenetic relationships based on SNPs dataset. We first reconstructed a ML tree based on concatenated 4339 SNPs using IQ-TREE with the same procedures as the above. We also performed a coalescent-based analysis to infer the species tree using the SVDQuartets (Chifman & Kubatko, 2014) implemented in PAUP v.4.0a149 (Swofford, 2002). For this analysis, we used 1590 unlinked SNPs with all possible quartets. Node support was assessed with 100 bootstrap replicates.

For species tree inferences using ASTRAL-III and SVDQuartets, we assigned samples to each of the six taxa (*R. thailandensis*, *R. yunanensis*, *R. p. chinensis*, and three clades of *R. p. pearsoni*, see Results).

2.5 Phylogenetic analysis on mtDNA

We also produced a ML tree based on the concatenated sequences of the 13 MPC genes using RAxML v8.2.12 (Stamatakis, 2014). This analysis was conducted with the GTRGAMMA model and bootstrap support was estimated based on 1000 pseudoreplicate searches. In this analysis, we included sequences of the 13 MPC genes from *R. ferrumequinum*, *R. sinicus* and *R. rex*, obtained from Mao et al. (2017) as outgroups.

2.6 Genetic structure and differentiation

We used two methods to assess population structure based on 2838 unlinked SNPs for all 82 ingroup individuals. First, we conducted an individual-based principal component analysis (PCA) using PLINK version-1.07 (Purcell et al., 2007), which was repeated for *R. p. pearsoni* individuals only in order to examine structure within this taxon. Second, we estimated individual assignment and genetic admixture using ADMIXTURE version 1.3 (Alexander et al., 2009). Admixture analysis was run with 10-fold cross-validation for a range of putative clusters (K=1 to 10). For each value of K, we conducted 10 independent runs, the results of which were combined in CLUMPAK (Kopelman et al., 2015). The most appropriate K value was selected based on the lowest average cross-validation (CV) error. Finally, genetic differentiation among the four chromosomal taxa was assessed using Fst (Weir & Cockerham, 1984) in VCFtools and P values of pairwise Fst were calculated using the R package StAMPP v1.6.3 (Pembleton et al., 2013).

2.7 Analysis of introgression

To detect any signatures of introgression among taxa we applied the D-statistic (ABBA-BABA) test (Durand et al., 2011; Green et al., 2010). This test examines the frequency of derived alleles (designated ‘B’) at loci that exhibit either an ABBA or BABA pattern in a four-taxon phylogeny: (((P1, P2), P3), outgroup) (Figure 3a). If only random lineage sorting of ancestral polymorphism take place, ABBA or BABA patterns are expected to occur at equal frequency (D-statistic = 0),

whereas a bias towards one pattern indicates potential introgression between P3 and either P1 or P2. Based on 16,164 SNPs with *R. thailandensis* 2n=60 as the outgroup, we used the Dtrios function in Dsuite version 0.5 (Malinsky et al., 2021) to estimate the D-statistic test for all possible three-taxon combinations in the species tree constructed by SVDquartets and ASTRAL above (Figure 3b). To test for introgression between *R. thailandensis* (P3) and other chromosomal taxa (P1 or P2) (Figure 3c), we also performed Dsuite analysis using *H. armiger* as the outgroup on the basis of 4339 SNPs. Statistical significance for the difference of the D-statistic value from zero was assessed by calculating the corresponding Z score using a standard block-jackknife procedure with different block sizes. To account for multiple tests, the adjusted p-value of 0.001 was used as the cutoff for significance of the D-statistic value after Benjamini and Hochberg adjustment (Benjamini & Hochberg, 1995).

To further estimate the relative magnitude and direction of introgression among taxa, while accounting for ILS, we used TreeMix version 1.13 (Pickrell & Pritchard, 2012). This analysis was based on 16,164 SNPs with *R. thailandensis* as the outgroup. A maximum likelihood tree with a migration edge (m) of zero was inferred and its likelihood was compared to ones of other ML trees with m of 1 to 5. For each migration edge, we used different SNPs windows (k=1, 10, 500) to account for the effect of linkage disequilibrium, which yielded same results. The optimal number of migration edges was determined using the R package OPTM (Fitak, 2021).

2.8 Phylogenetic network analysis

Finally, to infer phylogenies with reticulation events, we used PhyloNet 3.8.0 (Wen et al., 2018) to perform phylogenetic network analysis by accounting for both ILS and introgression. A maximum pseudolikelihood (MPL) approach was used with the command “InferNetwork_MPL”. Network analysis was performed based on a same set of 1153 gene trees as used in the ASTRAL analysis above. We tested for different number of reticulations (0-5) and each was performed with 20

independent searches using the parameters of –x –a –o. A bootstrap support threshold of 70 was applied with -b flag. The optimal network of each reticulation was visualized in Dendroscope3.8.3 (Huson & Scornavacca, 2012).

3. Results

For SNP calling, we first assembled a draft genome. Illumina sequencing yielded 126, 52, 36 and 32 Gb data for DNA libraries of 300 bp, 2k bp, 5k bp, and 10k bp, respectively (106, 45, 32, and 27 Gb data after trimming, Supp. Table S4). The draft genome assembly contains a total of 2.28 Gb with 73,147 scaffolds and its scaffold N50 was 330k bp (Supp. Table S5). BUSCO analysis revealed that 87.7% complete (S: 86.4%; D: 1.3%) and 4.3% fragmented BUSCOs were included in the draft genome (Supp. Table S6). Using target sequence capture, we generated datasets based on sequence alignments and SNPs. For sequence alignment datasets, we used 6458 nuclear exons of >250 bp each, and 1153 exons of >500 bp. We also obtained 13 MPC genes for all individuals. For the SNP datasets, we generated 16,164 SNPs (2838 unlinked) for ingroup individuals, and 4339 SNPs (1590 unlinked) for ingroup plus outgroup.

3.1 Phylogenetic relationships based on nuclear data

ML trees constructed separately using concatenated SNPs (n = 4339) and concatenated exons (n = 6458) showed similar topologies (Figure 2a and Supp. Figure S2). Here we described phylogenetic patterns based on the former. All four chromosomal taxa were reciprocally monophyletic with respect to each other (100 support rates). Of these, *R. thailandensis* (2n=60) and *R. yunanensis* (2n=46) showed early successive splits, and *R. p. pearsoni* (2n=44) and *R. p. chinensis* (2n=42) exhibited a sister relationship. Except for *R. p. pearsoni*, the other three chromosomal taxa had restricted distributions (Figure 1a). Within *R. p. pearsoni*, three separate clades were identified, with over 80 support rates (hereafter *R. p. pearsoni*-clade 1, clade 2 and clade 3). Among these, clade 1

diverged first, with members of this clade recorded in Hai Phong, Vietnam. Members of clade 2 were also from restricted regions (Hunan and Shanxi, locality of 9-12 in Figure 1a), whereas clade 3 had wide distributions ranging from China, Vietnam to Thailand (Figure 1a). To complement concatenation-based phylogenetic analyses, we also produced coalescent-based summary trees using ASTRAL and SVDQuartets based on 1153 exon alignments and 1590 unlinked SNPs, respectively. Both analyses recovered the same phylogenetic relationships among the four chromosomal taxa as revealed by concatenation (Figure 1d), however, within *R. p. pearsoni* (2n=44), coalescent methods supported a sister relationship between clade 1 and clade 3.

Consistent with results from phylogenetic analyses above, PCA based on 2838 unlinked SNPs for all ingroup individuals first separated *R. thailandensis* (2n=60) from others at PC1, which accounted for 59.4% of variance (Figure 1b). However, PC2 (18.5% variance) further separated *R. p. chinensis* (2n=42) from *R. p. pearsoni* (2n=44) and *R. yunanensis* (2n=46), supporting a closer relationship between *R. p. pearsoni* and *R. yunanensis*, contradicting the phylogenetic results. A second PCA for *R. p. pearsoni* also identified three separate clusters, corresponding to the three clades identified in the phylogenetic analyses.

Admixture analysis based on 2838 unlinked SNPs recovered the three chromosomal taxa (*R. thailandensis*, *R. yunanensis* and *R. p. chinensis*) and the three clades of *R. p. pearsoni* when run for K=6 (Figure 1c). The most likely number of clusters (i.e. lowest average CV error) was determined to be 7 (Supp. Figure S3), which recovered two clusters within clade 3 (Figure 1c). Consistent with results from phylogenetic analyses and PCA, *R. thailandensis* separated from the other bats at K=2, however, consistent with PCA result but in contrast to phylogenetic analyses, *R. p. chinensis* was the second to separate from *R. p. pearsoni* and *R. yunanensis* at K=3, supporting a closer relationship between *R. p. pearsoni* and *R. yunanensis*. Within *R. p. pearsoni*, individuals of clade 3 in Guizhou and Guangxi (locality of 15, 16 and 17 in Figure 1a and Supp. Table S1) were mixed with individuals from clade 2. It was notable that three individuals of *R. thailandensis* also mixed with *R.*

yunanensis.

Finally, pairwise Fst between the four chromosomal taxa also revealed *R. thailandensis* as the most divergent taxon with high Fst value (0.51-0.74) between *R. thailandensis* and each of the others (Figure 1d). In addition, genetic differentiation analysis also supported a closer relationship between *R. p. pearsoni* and *R. yunanensis* than between *R. p. pearsoni* and *R. p. chinensis* with Fst values of 0.16 and 0.25, respectively (Figure 1d).

3.2 Phylogenetic discordance between ncDNA and mtDNA

A concatenation-based ML tree using 13 MPC genes was consistent with ncDNA results, whereby *R. thailandensis* split first from the other taxa (Figure 2b). However, although *R. p. chinensis* and *R. yunanensis* were also identified as separated lineages with 100 support rates, these two taxa were nested within the *R. p. pearsoni*. Specifically, discordant with ncDNA results, *R. yunanensis* was classified with *R. p. pearsoni* clade 2 and some individuals of clade 3 from Guizhou (locality of 15 and 16) and Guangxi (locality of 17 in Figure 1a) where were near to the region of *R. yunanensis*. Similarly, *R. p. chinensis* was also classified with individuals of clade 2 and clade 3, although samples of clade 3 were far from the geographic range of *R. p. chinensis*. Finally, and in contrast to ncDNA results, clade 1 was not the most divergent lineage in *R. p. pearsoni* and was classified within clade 3.

3.3 Inference of introgression

We used two approaches to infer introgression. First, we used Dsuite to detect signatures of introgression by performing D-statistic tests for all possible three-taxon combinations. Dsuite analysis was first conducted under the species tree constructed by SVDquartets and ASTRAL and *R. thailandensis* as the outgroup (Figure 3b), which revealed five introgression events. Of these, three were between *R. yunanensis* and each of the three *R. p. pearsoni* clades (D=0.12, 0.11 and 0.12, see

Supp. Table S7). The others were between *R. p. chinensis* and *R. p. pearsoni* clade 2, and between *R. p. pearsoni* clade 2 and clade 3. To test for introgression between *R. thailandensis* and other chromosomal taxa, we performed a second Dsuite analysis with *H. armiger* as the outgroup (Figure 3c). Consistent with results of the Admixture analysis that several *R. thailandensis* individuals were mixed with *R. yunanensis* (Figure 1c), Dsuite analysis identified a signature of introgression between these two taxa (Supp. Table S7).We also used TreeMix, accounting for ILS, to estimate the relative magnitude and direction of introgression among taxa. The ML tree reconstructed by TreeMix revealed the same phylogenetic relationships among the six lineages (*R. thailandensis*, *R. yunanensis*, *R. p. chinensis*, and the three clades of *R. p. pearsoni*) as revealed in the species tree reconstructed by SVDquartets and ASTRAL. Under this ML tree, one migration event (m=1) was best supported by OptM and this introgression event was from *R. p. chinensis* into *R. p. pearsoni* clade 2 (Figure 3d).

3.4 Phylogenetic networks

Our observation of mitonuclear discordance and introgression analyses above both suggested occurrences of multiple introgression events among the four chromosomal taxa. To infer phylogenies with reticulation events, we used PhyloNet to perform phylogenetic network analysis. When reticulations were set to 1 and 2, the corresponding optimal networks (Figure 4) exhibited the same phylogenetic relationships among the four chromosomal taxa as revealed in the phylogenetic tree analyses (Figure 1e and 2a), while for reticulation of 3 to 5, the topologies were different from the phylogenetic tree analyses. In addition, the likelihood scores increase greatly from reticulation=0 to reticulation=1 and 2, followed by a gradual increase with more reticulations (Supp. Table S8 and Supp. Figure S4). Therefore, we only considered networks with one and two reticulation events, which best explain our current data. Both networks supported introgression between *R. thailandensis* and *R. yunanensis* and a second introgression event was inferred between *R. p. chinensis* and *R. p.*

pearsoni clade 2 when reticulation was set to 2 (Figure 4).

4. Discussion

Based on widespread sampling, our study included all four known chromosomal taxa of the *pearsoni* group (2n=42, 44, 46, 60). By performing phylogenetic, population genetic and introgression analyses on data of thousands of genomic loci, we demonstrated levels of diversification and introgression between the four chromosomal taxa. First, we reconstructed reliable phylogenetic relationships among the chromosomal taxa using phylogenetic tree and network methods by accounting for both ILS and introgression. Second, using different approaches, we detected multiple signatures of introgression between taxa and these introgression events might have occurred anciently. Below we discuss general implications of our results for diversification and introgression of closely related taxa with Rb changes.

4.1 Phylogenetic relationships among chromosomal taxa

Our phylogenetic analysis using both concatenation and coalescent methods supported a sister relationship between the two *R. pearsoni* subspecies (*R. p. chinensis* and *R. p. pearsoni*) to the exclusion of *R. yunanensis* (Figure 1e, 2a and Supp. Figure S2). However, results of population genetic analyses (PCA, Admixture and Fst estimates) all indicated that *R. p. pearsoni* had a closer relationship with *R. yunanensis* than with *R. p. chinensis* (Figure 1b-d, see details in Results), which can be best explained by introgression between *R. yunanensis* and *R. p. pearsoni* (see '*Introgression among chromosomal taxa*' below). To account for the effects of introgression between taxa on phylogenetic reconstruction, we also used TreeMix and PhyloNet to determine phylogenetic relationships between the chromosomal taxa. These two analysis approaches have been widely used to infer phylogeny while accounting for reticulation events (e.g. Ferreira et al., 2021; Hinojosa et al., 2022; Esquerré et al., 2022). The ML tree reconstructed by TreeMix (Figure 3d) and networks by

PhyloNet (Figure 4) both support the topology of ((*R. p. chinensis*, *R. p. pearsoni*), *R. yunanensis*) as revealed in the phylogenetic analyses. Thus, inference of the phylogenetic relationships using population genetic analyses might be not reliable when introgression had occurred, as shown in our case here. Our current study implies an importance of combining different analyses (e.g. phylogenetic, population genetic and network methods) in resolving phylogenetic relationships of closely related taxa with reticulation events, such as in the radiation of the *Heliconius* (Kozak et al., 2021) and *Petrogale* (Potter et al., 2022), and multiple chromosomal races of the house mouse on island (Franchini et al., 2020).

It was notable that ILS might also contribute to the genetic similarity between *R. yunanensis* and *R. p. pearsoni* observed in population genetic analyses. Even with the analyses of genome-wide data, it is now still difficult to distinguish the relative effects of ILS and introgression on phylogenetic reconstruction (e.g. Meleshko et al., 2021; Lopes et al., 2021). However, in this study, results of the ABBA-BABA tests in Dsuite and TreeMix, both accounting for ILS, suggested that introgression scenario was more likely. In the future, a method of quantifying introgression via branch length (QuIBL) (Edelman et al., 2019) can be applied to the whole genome sequencing data to further test for the relative effects of introgression and ILS in phylogenetic discordances among the three chromosomal taxa.

Finally, the wide geographical sampling of bats in this study has revealed inconsistent taxonomic assignments in earlier work. In particular, some samples of *R. p. pearsoni* clade 3 and *R. yunanensis* in this study (see below) were previously recognized as '*R. yunanensis*' and '*R. p. pearsoni*', respectively (Mao et al., 2010). *Rhinolophus yunanensis* and *R. pearsoni* have long been confused and their close morphological similarity means that they are likely to be frequently misidentified in the field. Indeed, it is noteworthy that bats from Cambodia and Thailand that were analysed in this study were previously classified as *R. yunanensis* by fieldworkers (Supp. Table S1). In light of our new results, which are based on wide sampling of taxa in the *pearsoni* complex, alongside karyotype

data (Wu et al., 2009) and genetic variation (Figure 2), we suggest that samples from Sichuan are more likely to be ascribed to *R. yunanensis*, further highlighting the importance of combining different sources of data for correct species recognition. Currently, karyotype data are lacking for most populations of the *pearsoni* group. Ultimately, it will be important to determine whether some genetically divergent lineages in this group belong to different chromosomal taxa, such as populations from Hai Phong in Vietnam, Songkhla in Thailand and Kampot in Cambodia.

4.2 Introgression among chromosomal taxa

Our analyses using Dsuite, TreeMix and PhyloNet all supported introgression between *R. p. chinensis* (2n=42) and *R. p. pearsoni* clade 2 (2n=44), which was also suggested by the detection of mitonuclear discordance here (see details in Results) and in a previous study based on mtDNA and two nuclear loci (Mao et al., 2010). Nuclear introgression between these two subspecies has also been inferred based on gene flow analysis of multiple nuclear loci (Mao et al., 2016). However, despite these findings, our PCA and admixture analyses both pointed to a lack of recent or ongoing introgression, and introgressed *R. p. pearsoni* mtDNA sequences were seen to be highly divergent from those of *R. p. chinensis* (Figure 2b), again consistent with no recent hybridization and mtDNA introgression. Although phenotypic differences are not a focus of this study, the cessation of gene flow between *R. p. pearsoni* and *R. p. chinensis* is further supported by divergence in their echolocation call frequencies (~10 kHz difference, Mao et al., 2010). Previous work has found a link between call frequency divergence and negative assortative mating, implying possible prezygotic isolation (Kingston & Rossiter, 2004; Puechmaille et al., 2014). At the same time, it is not known whether such call frequency divergence is directly related to chromosomal differences observed between our study taxa, although chromosomal variation has previously been linked to local adaptation in salmon (Wellband et al., 2019) and trait divergence in deer mice (Hager et al., 2022). Indeed, previous studies of house mice suggested an important role of Rb fusions specifically in

phenotypic divergence (Franchini et al., 2016). Future chromosome-level genome assemblies alongside whole genome resequencing will be important in testing roles of chromosomal changes in isolation between chromosomal taxa, including structural rearrangements such as translocations and inversions, in addition to Rb changes (e.g. Moran et al., 2020; Cheng et al., 2021; Huang et al., 2022). Similarly, genome scans and genome-wide associated studies (GWAS) may also offer opportunities to identify candidate genomic loci associated with phenotypic variation and/or reproductive isolation, including whether or not they are located within rearranged regions (e.g. Jackson et al., 2021; Mérot et al., 2022).

Using the D-statistic test in Dsuite, we also found evidence of substantial past introgression between *R. yunanensis* (2n=46) and each of the three clade of *R. p. pearsoni* (2n=44), although this was not recovered by TreeMix and PhyloNet. Based on the parsimony principle for inferring possible introgression events (Pulido-Santacruz et al., 2020; Zhang et al., 2021), we proposed that a single introgression event might have occurred between *R. yunanensis* and the ancestor of *R. p. pearsoni*. The classification of *R. yunanensis* with *R. p. pearsoni* clade 3 from Guangxi and Guizhou (locality of 15, 16 and 17 in Figure 1a) in the mtDNA tree (Figure 1a and 2b) also supported an occurrence of hybridization and introgression between them.

Similarly, a closer relationship between *R. p. pearsoni* and *R. yunanensis* than between *R. p. pearsoni* and *R. p. chinensis*, as revealed in the PCA, Admixture and Fst analyses, also supported a scenario of introgression. Yet, like the results for *R. p. pearsoni* and *R. p. chinensis*, no recent and ongoing introgression was detected between *R. yunanensis* and any clade of *R. p. pearsoni*, a result further supported by the separation of *R. yunanensis* into a monophyletic clade in the mtDNA tree (Figure 2b). Similar examples of ancient introgression between a taxon and the ancestor of a set of other taxa have previously been reported in other study systems, including fishes (Meier et al., 2017), birds (Zhang et al., 2021) and plants (Meleshko et al., 2021). Once again, whole genome sequencing in the future will help to shed light on the extent and timing of introgression between *R.*

p. pearsoni and *R. yunanensis*.

Finally, we found unexpected evidence of introgression between *R. thailandensis* (2n=60) and *R. yunanensis* (2n=46) using Admixture (Figure 1c), the D-statistics test (Figure 3c) and network analysis (Figure 4). These results seem to suggest that even complex Rb changes (at least seven fusions/fissions here) may not impede introgression, a result also documented in the rock-wallaby group (Potter et al., 2022) and the common shrew (Polyakov et al., 2011; Horn et al., 2012). Because *R. thailandensis* is only reported in the Chiang Mai area of Thailand (Wu et al., 2009; Bouillard, 2021), such introgression may well have occurred between *R. thailandensis* and a more widely distributed ancestor of *R. yunanensis*. Additional sampling of *R. yunanensis* in Thailand, together with karyotyping and genome sequencing, will help address the question of whether there are *R. yunanensis* individuals with 2n=46 in Thailand, and the level of diversification and introgression between these *R. yunanensis* individuals and *R. thailandensis*.

Overall, we have discovered multiple signatures of ancient introgression between four chromosomal taxa that differ by one or more Rb changes. Our current results thus seem to support the idea that Rb changes have little effect on the fertility of hybrids and thus may play a minor role in causing reproductive isolation, as observed in house mice (Garagna et al., 2014; Grize et al., 2019), shrews (Searle et al., 2019) and rock-wallabies (Potter et al., 2022). At the same time, no recent and/or ongoing introgression was observed between these three chromosomal taxa (2n=42, 44 and 46), implying that simple chromosomal changes may also reduce introgression and promote isolation. One possible explanation for this discrepancy is that the legacy of ancient introgression events involving ancestral taxa will be easier to detect since they will likely be seen at broader geographical scales, reflecting the ranges of the descendant taxa, as opposed to recent events involving single extant populations, which are less likely to be sampled. Alternatively, this discrepancy could be explained by ancient introgression events among individuals with chromosome polymorphisms, in which gene flow ceased after fixation of chromosome differences. Thus, our work is consistent with

the findings in other organism systems (Potter et al., 2022; Franchini et al., 2020) that the effects of Rb changes on the reduction of introgression are complicated and Rb changes may contribute to speciation together with other factors (e.g. genic evolution).

A more robust way to test whether Rb changes have consequences for diversification and introgression would be to compare introgression rates between groups of taxa that differ with respect to Rb changes but which show similar divergence times; however, this latter condition is not met by our study group. In the future, chromosome-level sequence alignments and whole genome resequencing will likely provide better insights into the extent of rearrangements (e.g. translocations and inversions) as well as the timing of introgression (e.g. Hibbins & Hahn, 2018). In particular, comparing the timing of chromosomal changes between the chromosomal taxa will provide information on whether introgression occurred before or after the formation of chromosomal changes, and thus whether chromosomal changes might have contributed to reproductive isolation, or accumulated subsequently (Faria & Navarro, 2010). More importantly, the four chromosomal taxa studied here, in particular the two closely related *R. pearsoni* subspecies (*R. p. chinensis* and *R. p. pearsoni*), can be used as a good system to investigate the molecular mechanisms of chromosomal speciation (e.g. Yin et al., 2021). Together with the identification of candidate loci associated with phenotypic divergence (e.g. call frequency divergence between the two *R. pearsoni* subspecies), whole genome sequencing data will be needed to test for the role chromosomal rearrangements in ecological speciation (e.g. Jackson et al., 2021).

Authors' contributions. XM and SR conceived the project; WZ analysed the data; NF, PC, VT and BL provided samples; XM wrote the draft of the manuscript with the help of WZ and SR; XM and SR edited the manuscript.

Competing interests. We declare we have no competing interests.

Funding. This work was supported by a European Research Council Starting Grant 310482 (EVOGENO) to SJR and a Marie Curie International Incoming Fellowship for X Mao. X Mao was also supported by the grant from The Scientific and Technological Innovation Plan of Shanghai Science and Technology Committee (20ZR1417000). Vu Dinh Thong was supported by the Vietnam Academy of Science and Technology under grant number VAST04.03/21-22.

ACKNOWLEDGEMENTS. We thank Georgia Tsagkogeorga for her help in assembling the draft genome and three anonymous reviewers for constructive comments that improved the manuscript.

References

Alexander, D. H., Novembre, J., Lange, K. 2009 Fast model-based estimation of ancestry in unrelated individuals. Genome Res, 19, 1655-1664. (DOI:10.1101/gr.094052.109)

Andermann, T., Cano, Á., Zizka, A., Bacon, C., Antonelli, A. 2018 SECAPR—a bioinformatics pipeline for the rapid and user-friendly processing of targeted enriched Illumina sequences, from raw reads to alignments. PeerJ, 6, e5175. (DOI:10.1093/sysbio/syy039)

Andrews, S. 2010 FastQC: a quality control tool for high throughput sequence data. Retrieved from https://www.bioinformatics.babraham. ac.uk/projects/fastqc/

Ao, L et al. 2007 Karyotypic evolution and phylogenetic relationships in the order Chiroptera as revealed by G-banding comparison and chromosome painting. Chromosome Res, 15, 257-268. (DOI:10.1007/s10577-007-1120-7)

Ayala, F. J., Coluzzi, M. 2005 Chromosome speciation: humans, Drosophila, and mosquitoes. Proc. Natl. Acad. Sci. 102, 6535-6542. (DOI:10.1073/pnas.0501847102)

Bailey, S. E et al. 2016 The use of museum samples for large-scale sequence capture: a study of congeneric horseshoe bats (family Rhinolophidae). Biol J Linn Soc, 117, 58-70. (DOI: 10.1111/bij.12620)

Bankevich, A et al. 2012 SPAdes: a new genome assembly algorithm and its applications to single-cell sequencing. J Comput Biol, 19, 455-477. (DOI:10.1089/cmb.2012.0021)

Bates, P.J.J., Bumrungsri, S., Csorba, G. Mao, X.G. 2019 *Rhinolophus pearsonii*. The IUCN Red List of Threatened Species 2019:e.T19559A21993105.(DOI:10.2305/IUCN.UK.2019-3.RLTS.T19559A21993105.en)

Bates, P.J.J., Bumrungsri, S., Csorba, G., Molur, S., Srinivasulu, C. Mao, X.G. 2019 *Rhinolophus yunanensis*. The IUCN Red List of Threatened Species 2019: e.T19576A21991423.(DOI:10.2305/IUCN.UK.2019-3.RLTS.T19576A21991423.en)

Benjamini, Y., Hochberg, Y. 1995 Controlling the false discovery rate: a practical and powerful approach to multiple testing. J R Stat Soc B, 57, 289-300. (DOI:10.1111/j.2517-6161.1995.tb02031.x)

Bolger, A.M., Lohse, M., Usadel, B. 2014 Trimmomatic: a flexible trimmer for Illumina sequence data, Bioinformatics, 30, 2114–2120. (DOI:10.1093/bioinformatics/btu170)

Bouillard, N. 2021 *Rhinolophus thailandensis*. The IUCN Red List of Threatened Species 2021:e.T82348077A82348673.(DOI:10.2305/IUCN.UK.2021-2.RLTS.T82348077A82348673.en)

Capella-Gutiérrez, S., Silla-Martínez, J. M., Gabaldón, T. 2009 trimAl: a tool for automated alignment trimming in large-scale phylogenetic analyses. Bioinformatics, 25, 1972-1973. (DOI:10.1093/bioinformatics/btp348)

Charron, G., Leducq, J. B., Landry, C. R. 2014 Chromosomal variation segregates within incipient species and correlates with reproductive isolation. Mol. Ecol. 23, 4362-4372. (DOI:10.1111/mec.1/2864)

Cheng, P et al. 2021 The American paddlefish genome provides novel insights into chromosomal evolution and bone mineralization in early vertebrates. Mol Biol Evol, 38, 1595-1607. (DOI:10.1093/molbev/msaa326)

Chifman, J., Kubatko, L. 2014 Quartet inference from SNP data under the coalescent model. Bioinformatics, 30, 3317-3324. (DOI:10.1093/bioinformatics/btu530)

Cicconardi, F., Lewis, J. J., Martin, S. H., Reed, R. D., Danko, C. G., Montgomery, S. H. 2021 Chromosome fusion affects genetic diversity and evolutionary turnover of functional loci but consistently depends on chromosome size. Mol. Biol. Evol. 38, 4449-4462. (DOI:10.1093/molbev/msab185)

Danecek, P et al. 2011 The variant call format and VCFtools. Bioinformatics, 27, 2156-2158. (DOI:10.1093/bioinformatics/btr330)

de Vos, J. M., Augustijnen, H., Bätscher, L., Lucek, K. 2020 Speciation through chromosomal fusion

and fission in Lepidoptera. Philos. Trans. R. Soc. Lond., B, Biol. Sci, 375, 20190539. (DOI:10.1098/rstb.2019.0539)
Dobzhansky, T., Dobzhansky, T. G. 1971 Genetics of the evolutionary process (Vol. 139). Columbia University Press.
Durand, E. Y., Patterson, N., Reich, D., Slatkin, M. 2011 Testing for ancient admixture between closely related populations. Mol Biol Evol, 28, 2239-2252. (DOI:10.1093/molbev/msr048)
Edelman, N. B et al. 2019 Genomic architecture and introgression shape a butterfly radiation. Science, 366, 594-599. (DOI:10.1101/466292)
Esquerré, D et al. 2022 Rapid radiation and rampant reticulation: Phylogenomics of South American *Liolaemus* lizards. Syst Biol, 71, 286-300. (DOI:10.1093/sysbio/syab058)
Faria, R., Navarro, A. 2010 Chromosomal speciation revisited: rearranging theory with pieces of evidence. Trends Ecol. Evol. 25, 660-669. (DOI:10.1016/j.tree.2010.07.008)
Ferreira, M. S et al. 2021 The legacy of recurrent introgression during the radiation of hares. Syst Biol, 70, 593-607. (DOI:10.1093/sysbio/syaa088)
Fitak, R. R. 2021 OptM: estimating the optimal number of migration edges on population trees using Treemix. Bio Methods Protoc, 6, bpab017. (DOI:10.1093/biomethods/bpab017)
Foll, M., Gaggiotti, O. 2008 A genome-scan method to identify selected loci appropriate for both dominant and codominant markers: a Bayesian perspective. Genetics, 180, 977-993. (DOI:10.1534/genetics.108.092221)
Franchini, P., Colangelo, P., Meyer, A., Fruciano, C. 2016 Chromosomal rearrangements, phenotypic variation and modularity: a case study from a contact zone between house mouse Robertsonian races in Central Italy. Ecol Evol, 6, 1353-1362. (DOI:10.1002/ece3.1912)
Franchini, P., Kautt, A. F., Nater, A., Antonini, G., Castiglia, R., Meyer, A., Solano, E. 2020 Reconstructing the evolutionary history of chromosomal races on islands: a genome-wide analysis of natural house mouse populations. Mol. Biol. Evol, 37, 2825-2837. (DOI:10.1093/molbev/msaa118)
Garagna, S., Page, J., Fernandez-Donoso, R., Zuccotti, M., Searle, J. B. 2014 The Robertsonian phenomenon in the house mouse: mutation, meiosis and speciation. Chromosoma, 123, 529-544. (DOI:10.1007/s00412-014-0477-6)
Giménez, M. D et al. 2017 A half-century of studies on a chromosomal hybrid zone of the house mouse. J. Hered, 108, 25-35. (DOI:10.1093/jhered/esw061)
Green, R. E et al. 2010 A draft sequence of the Neandertal genome. Science, 328, 710-722. (DOI:10.1126/science.1188021)
Grize, S. A., Wilwert, E., Searle, J. B., Lindholm, A. K. 2019 Measurements of hybrid fertility and a test of mate preference for two house mouse races with massive chromosomal divergence. BMC Evol. Biol, 19, 25. (DOI:10.1186/s12862-018-1322-y)
Hager, E. R et al. 2022 A chromosomal inversion contributes to divergence in multiple traits between deer mouse ecotypes. Science, 377, 399-405. (DOI:10.1126/science.abg0718)
Harada, M., Yenbutra, S., Yosida, T. H., Takada, S. 1985 Cytogenetical study of *Rhinolophus* bats (Chiroptera, Mammalia) from Thailand. P Jpn Acad, Series B, 61, 455-458. (DOI:10.2183/pjab.61.455)
Hibbins, M. S., Hahn, M. W. 2018 Population genetic tests for the direction and relative timing of introgression. BioRxiv, 328575. (DOI:10.1101/328575)
Hinojosa, J. C et al. 2022 Hybridization fuelled diversification in *Spialia* butterflies. Mol Ecol, 31, 2951-2967. (DOI:10.1111/mec.16426)
Hoang, D. T., Chernomor, O., Von Haeseler, A., Minh, B. Q., Vinh, L. S. 2018 UFBoot2: improving the ultrafast bootstrap approximation. Mol. Biol. Evol, 35, 518-522. (DOI:10.1093/molbev/msx281)
Horn, A et al. 2012 Chromosomal rearrangements do not seem to affect the gene flow in hybrid zones between karyotypic races of the common shrew (*Sorex araneus*). Evolution, 66, 882-889. (DOI:10.1111/j.1558-5646.2011.01478.x)
Huang, Z et al. 2022 Recurrent chromosome reshuffling and the evolution of neo-sex chromosomes

in parrots. Nat Commun, 13, 1-11. (DOI:10.1101/2021.03.08.434498)
Huson, D. H., Scornavacca, C. 2012 Dendroscope 3: an interactive tool for rooted phylogenetic trees and networks. Syst Biol, 61, 1061-1067. (DOI:10.1093/sysbio/sys062)
Hutson, A. M., S. Rossiter, G. Csorba, C. Burgin. 2019 "Family Rhinolophidae (horseshoe bats)." Handbook of the Mammals of the World: Bats. Lynx Edicions, Spain, 1008pp: 260-332.
Jackson, C. E., Xu, S., Ye, Z., Pfrender, M. E., Lynch, M., Colbourne, J. K., Shaw, J. R. 2021 Chromosomal rearrangements preserve adaptive divergence in ecological speciation. BioRxiv. (DOI:10.1101/2021.08.20.457158)
Kalyaanamoorthy, S., Minh, B. Q., Wong, T. K., Von Haeseler, A., Jermiin, L. S. 2017 ModelFinder: fast model selection for accurate phylogenetic estimates. Nat. Methods, 14, 587-589. (DOI:10.1038/nmeth.4285)
Katoh, K., Misawa, K., Kuma, K. I., Miyata, T. 2002 MAFFT: a novel method for rapid multiple sequence alignment based on fast Fourier transform. Nucleic Acids Res, 30, 3059-3066.
King, M. 1995 Species evolution: the role of chromosome change. Cambridge University Press.
Kingston, T., Rossiter, S. J. 2004 Harmonic-hopping in Wallacea's bats. Nature, 429, 654-657. (DOI:10.1038/nature02487)
Kopelman, N. M., Mayzel, J., Jakobsson, M., Rosenberg, N. A., Mayrose, I. 2015 Clumpak: a program for identifying clustering modes and packaging population structure inferences across K. Mol Ecol Res, 15, 1179-1191. (DOI:10.1111/1755-0998.12387
Kozak, K. M., Joron, M., McMillan, W. O., Jiggins, C. D. 2021 Rampant genome-wide admixture across the *Heliconius* radiation. Genome Biol Evol, 13, evab099. (DOI:10.1093/gbe/evab099)
Leducq, J. B et al. 2016 Speciation driven by hybridization and chromosomal plasticity in a wild yeast. Nat Microbiol, 1, 15003. (DOI:10.1101/027383)
Li, H. 2011 A statistical framework for SNP calling, mutation discovery, association mapping and population genetical parameter estimation from sequencing data. Bioinformatics, 27, 2987–2993. (DOI:10.1093/bioinformatics/btr509)
Li, H., Durbin, R. 2010 Fast and accurate long-read alignment with Burrows–Wheeler transform. Bioinformatics, 26, 589-595. (DOI:10.1093/bioinformatics/btp698)
Li, H et al. 2009 The sequence alignment/map format and SAMtools. Bioinformatics, 25, 2078-2079. (DOI:10.1093/bioinformatics/btp352)
Liu, Z., Roesti, M., Marques, D., Hiltbrunner, M., Saladin, V., Peichel, C. L. 2022 Chromosomal fusions facilitate adaptation to divergent environments in threespine stickleback. Mol. Biol. Evol, 39, msab358. (DOI:10.1093/molbev/msab358)
Lopes, F et al. 2021 Phylogenomic discordance in the eared seals is best explained by incomplete lineage sorting following explosive radiation in the southern hemisphere. Syst Biol, 70, 786-802. (DOI:10.1093/sysbio/syaa099)
Lucek, K., Augustijnen, H., Escudero, M. 2022 A holocentric twist to chromosomal speciation? Trends Ecol. Evol. 37, 655-662. (DOI:10.1016/j.tree.2022.04.002)
Lukhtanov, V. A., Shapoval, N. A., Anokhin, B. A., Saifitdinova, A. F., Kuznetsova, V. G. 2015 Homoploid hybrid speciation and genome evolution via chromosome sorting. Proc. Royal Soc. B, 282, 20150157. (DOI:10.1098/rspb.2015.0157)
Luo, R et al. 2012 SOAPdenovo2: an empirically improved memory-efficient short-read de novo assembler. Gigascience, 1, 2047-217X.
Malinsky, M., Matschiner, M., Svardal, H. 2021 Dsuite□Fast D□statistics and related admixture evidence from VCF files. Mol Ecol Res, 21, 584-595. (DOI:10.1111/1755-0998.13265)
Manichaikul, A., Mychaleckyj, J. C., Rich, S. S., Daly, K., Sale, M., Chen, W. M. 2010 Robust relationship inference in genome-wide association studies. Bioinformatics, 26, 2867-2873. (DOI: 10.1093/bioinformatics/btq559)
Mao, X et al. 2007 Karyotype evolution in *Rhinolophus* bats (Rhinolophidae, Chiroptera) illuminated by cross-species chromosome painting and G-banding comparison. Chromosome Res,

15, 835-848. (DOI:10.1007/s10577-007-1167-5)
Mao, X et al. 2008 Comparative cytogenetics of bats (Chiroptera): the prevalence of Robertsonian translocations limits the power of chromosomal characters in resolving interfamily phylogenetic relationships. Chromosome Res, 16, 155-170. (DOI:10.1007/s10577-007-1206-2)
Mao, X., Rossiter, S. J. 2020 Genome-wide data reveal discordant mitonuclear introgression in the intermediate horseshoe bat (*Rhinolophus affinis*). Mol Phylogenet and Evol, 150, 106886. (DOI: 10.1016/j.ympev.2020.106886)
Mao, X., Tsagkogeorga, G., Bailey, S. E., Rossiter, S. J. 2017 Genomics of introgression in the Chinese horseshoe bat (*Rhinolophus sinicus*) revealed by transcriptome sequencing. Biol J Linn Soc, 121, 698-710. (DOI: 10.1093/biolinnean/blx017)
Mao, X., Tsagkogeorga, G., Thong, V. D., Rossiter, S. J. 2019 Resolving evolutionary relationships among six closely related taxa of the horseshoe bats (*Rhinolophus*) with targeted resequencing data. Mol Phylogenet Evol, 139, 106551. (DOI: 10.1016/j.ympev.2019.106551)
Mao, X., Zhang, J., Zhang, S., Rossiter, S. J. 2010 Historical male□mediated introgression in horseshoe bats revealed by multilocus DNA sequence data. Mol Ecol, 19, 1352-1366. (DOI: 10.1111/j.1365-294X.2010.04560.x)
Mao, X., Zhang, S., Rossiter, S. J. 2016 Differential introgression suggests candidate beneficial and barrier loci between two parapatric subspecies of Pearson's horseshoe bat *Rhinolophus pearsoni*. Curr Zool, 62, 405-412. (DOI: 10.1093/cz/zow017)
Meier, J. I., Marques, D. A., Mwaiko, S., Wagner, C. E., Excoffier, L., Seehausen, O. 2017 Ancient hybridization fuels rapid cichlid fish adaptive radiations. Nat commun, 8, 1-11. (DOI:10.1038/ncomms14363)
Meleshko, O et al. 2021 Extensive genome-wide phylogenetic discordance is due to incomplete lineage sorting and not ongoing introgression in a rapidly radiated bryophyte genus. Mol Biol Evol, 38, 2750-2766. (DOI: 10.1093/molbev/msab063)
Mérot, C et al. 2022 Genome assembly, structural variants, and genetic differentiation between lake whitefish young species pairs (*Coregonus sp*.) with long and short reads. BioRxiv. (DOI: 10.1101/2022.01.15.476463)
Moran, R. L., Catchen, J. M., Fuller, R. C. 2020 Genomic resources for darters (Percidae: Etheostominae) provide insight into postzygotic barriers implicated in speciation. Mol Biol Evol, 37, 711-729. (DOI:10.1093/molbev/msz260)
Morni, M. A et al. 2016 New record of *Rhinolophus chiewkweeae* (Chiroptera: Rhinolophidae) from the east coast of Peninsular Malaysia with new information on their echolocation calls, genetics and their taxonomy. RAFFLES B ZOOL, 64, 242–249.
Navarro, A., Barton, N. H. 2003 Chromosomal speciation and molecular divergence--accelerated evolution in rearranged chromosomes. Science, 300, 321-324. (DOI: 10.1126/science.1080600)
Nguyen, L. T., Schmidt, H. A., Von Haeseler, A., Minh, B. Q. 2015 IQ-TREE: a fast and effective stochastic algorithm for estimating maximum-likelihood phylogenies. Mol. Biol. Evol, 32, 268-274. (DOI: 10.1093/molbev/msu300)
Pickrell, J., Pritchard, J. 2012 Inference of population splits and mixtures from genome-wide allele frequency data. PLoS Genet. 8, e1002967. (DOI: 10.1371/journal.pgen.1002967)
Polyakov, A. V., White, T. A., Jones, R. M., Borodin, P. M., Searle, J. B. 2011 Natural hybridization between extremely divergent chromosomal races of the common shrew (*Sorex araneus*, Soricidae, Soricomorpha): hybrid zone in Siberia. J Evolution Biol, 24, 1393-1402. (DOI: 10.1111/j.1420-9101.2011.02266.x)
Potter, S., Bragg, J. G., Blom, M. P., Deakin, J. E., Kirkpatrick, M., Eldridge, M. D., Moritz, C. 2017 Chromosomal speciation in the genomics era: disentangling phylogenetic evolution of rock-wallabies. Front. Genet. 8:10. (DOI:10.3389/fgene.2017.00010)
Potter, S et al. 2022 Limited introgression between rock-wallabies with extensive chromosomal rearrangements. Mol. Biol. Evol, 39, msab333. (DOI: 10.1093/molbev/msab333)

Puechmaille, S. J et al. 2014 Female mate choice can drive the evolution of high frequency echolocation in bats: a case study with *Rhinolophus mehelyi*. PloS One, 9, e103452. (DOI: 10.1371/journal.pone.0103452)
Pulido□Santacruz, P., Aleixo, A., Weir, J. T. 2020 Genomic data reveal a protracted window of introgression during the diversification of a Neotropical woodcreeper radiation. Evolution, 74, 842-858. (DOI:10.1111/evo.13902)
Purcell et al. 2007 PLINK: a tool set for whole-genome association and population-based linkage analyses. Am. J. Hum. Genet, 81, 559-575. (DOI: \10.1086/519795)
Rieseberg, L. H. 2001 Chromosomal rearrangements and speciation. Trends Ecol. Evol. 16, 351-358. (DOI:10.1016/S0966-842X(00)01826-6)
Rieseberg, L. H., Livingstone, K. 2003 Chromosomal speciation in primates. Science, 300, 267-268. (DOI:10.1126/science.1084192)
Schwartz, S et al. 2003 Human–mouse alignments with BLASTZ. Genome Res, 13, 103-107. (DOI: 10.1101/gr.809403)
Searle J. B. 1993 Chromosomal hybrid zones in eutherian mammals. Hybrid zones and the evolutionary process (ed. RG Harrison). Oxford University Press, Oxford. pp. 309-353
Searle, J. B., Polly, P. D., Zima, J. 2019 Shrews, chromosomes and speciation (Vol. 6) (Eds.). Cambridge University Press. pp. 365–383 (DOI: 10.1017/9780511895531)
Simão, F. A., Waterhouse, R. M., Ioannidis, P., Kriventseva, E. V., Zdobnov, E. M. 2015 BUSCO: assessing genome assembly and annotation completeness with single-copy orthologs. Bioinformatics, 31, 3210-3212. (DOI: 10.1093/bioinformatics/btv351)
Simmons, N. B., Cirranello, A. L. 2020 Bat Species of the World: A taxonomic and geographic database. Retrieved from: https://www.batnames.org/.
Sotero-Caio, C. G., Baker, R. J., Volleth, M. 2017 Chromosomal evolution in Chiroptera. Genes, 8, 272. (DOI: 10.3390/genes8100272)
Stamatakis, A. 2014 RAxML version 8: a tool for phylogenetic analysis and post-analysis of large phylogenies. Bioinformatics, 30, 1312-1313. (DOI: 10.1093/bioinformatics/btu033)
Swofford, D. L. 2002 PAUP: phylogenetic analysis using parsimony (and other methods), 4.0 beta. Retrieved from: http://paup. csit. fsu. edu/. (DOI: 10.1002/0471650129.dob0522)
Waldien, D.L. 2020 *Rhinolophus chiewkweeae*. The IUCN Red List of Threatened Species 2020:e.T84372474A84372528.(DOI:10.2305/IUCN.UK.2020-2.RLTS.T84372474A84372528.en)
Weir, B. S., Cockerham, C. C. 1984 Estimating F-statistics for the analysis of population structure. Evolution, 38, 1358-1370. (DOI: 10.1111/j.1558-5646.1984.tb05657.x)
Wellband, K., Mérot, C., Linnansaari, T., Elliott, J. A. K., Curry, R. A., Bernatchez, L. 2019 Chromosomal fusion and life history□associated genomic variation contribute to within□river local adaptation of Atlantic salmon. Mol. Ecol. 28, 1439-1459. (DOI: 10.1101/347724)
Wen, D., Yu, Y., Zhu, J., Nakhleh, L. 2018 Inferring phylogenetic networks using PhyloNet. Syst Biol, 67, 735-740. (DOI: 10.1101/238071)
White, M.J.D. 1978 Modes of Speciation. pp.478–482. W. II. Freeman. San Francisco.
Wu, Y., Harada, M., Motokawa, M. 2009 Taxonomy of *Rhinolophus yunanensis* Dobson, 1872 (Chiroptera: Rhinolophidae) with a description of a new species from Thailand. Acta Chiroptero, 11, 237-246. (DOI:10.3161/150811009X485486)
Wu, Y., Harada, M., Shi, H., Liu, H. 2006 Further study on karyology of bats (Mammalia: Chiroptera) from Sichuan, China. Journal of Guangzhou University (Natural Science Edition), 5: 20–24
Yin, Y et al. 2021 Molecular mechanisms and topological consequences of drastic chromosomal rearrangements of muntjac deer. Nat Commun, 12, 1-15. (DOI: 10.1038/s41467-021-27091-0)
Yoshiyuki, M., Lim, B. L. 2005 A new horseshoe bat, *Rhinolophus chiewkweeae* (Chiroptera, Rhinolophidae), from Malaysia. Bull. Natl. Sci. Mus. Tokyo, Series A, 31, 29-36.
Zhang, C., Rabiee, M., Sayyari, E., Mirarab, S. 2018 ASTRAL-III: polynomial time species tree

reconstruction from partially resolved gene trees. BMC Bioinform, 19, 15-30. (DOI: 10.1186/s12859-018-2129-y)
Zhang, D et al. 2021 Most genomic loci misrepresent the phylogeny of an avian radiation because of ancient gene flow. Syst Biol, 70, 961-975. (DOI: 10.1093/sysbio/syab024)
Zhang, W. 1985 A study on the karyotypes in four species of bat (*Rhinolophus*). Shou Lei Xue Bao, 5, 95–101.
Zima, J., Volleth, M., Horácek, I., Cerveny, J., Cervena, A., Prucha, K., Macholan, M. 1992 Comparative karyology of rhinolophid bats (Chiroptera: Rhinolophidae). Prague Studies in Mammalogy, Charles University Press, 229–236

Figure legends

Figure 1. (a) A map showing sampling localities in this study and approximate ranges of the four species in the *Rhinolophus pearsoni* group. Taxa memberships of individuals in each location are based on the results of clustering (b and c) and phylogenetic analyses (e and Figure 2a). (b) PCAs results for all 82 ingroup individuals and only *R. p. pearsoni* individuals based on 2838 SNPs, respectively. Individuals were classified into six clusters, *R. thailandensis*, *R. yunanensis*, *R. p. chinensis* and three clades of *R. p. pearsoni*. (c) K=6 and 7 from ADMIXTURE results for all 82 ingroup individuals based on 2838 SNPs. Six clusters when K=6 match those identified in the PCAs. A further cluster was observed within *R. p. pearsoni* clade 3 when K=7. (d) Fst results between pairwise comparisons of the four chromosomal taxa. * indicates that all Fst values were significant with P-value <0.05. (e) Inference of the species tree using SVDquartets and ASTRAL based on 1590 SNPs and 1153 gene trees, respectively. Numbers in each branch represent bootstrap values from SVDquartets (above the branch) and posterior probabilities from ASTRAL (below the branch). *Hipposideros armiger* was used as the outgroup. Taxa are colored according to those in the PCAs and Admixture analyses.

Figure 2. Phylogenetic trees based on nuclear DNA (ncDNA, a) and mitochondrial DNA (mtDNA, b). NcDNA tree was inferred based on concatenated 4354 nuclear SNPs using IQtree and mtDNA tree based on concatenated 13 mitochondrial protein-coding genes using RAxML. The numbers on branches indicate the bootstrap support values.

Figure 3. Introgression analysis results. (a) A diagram showing an example of the D-statistic test. (b) The D-statistic test results using *R. thailandensis* as the outgroup under the species tree topology. (c) The D-statistic test results using *Hipposideros armiger* as the outgroup under the species tree topology. (d) TreeMix results for the most likely number of introgression event (m=1) and selection of the most likely number of migration edges by the OptM R package. The arrow indicates relative magnitude and direction of introgression from *R. p. chinensis* into *R. p. pearsoni* clade 2. Six taxa match those in the species tree (see Figure 1e). *R. thailandensis* was used as the outgroup.

Figure 4. Phylogenetic networks estimated using PhyloNet with reticulation of 1 and 2. Blue lines represent the reticulation event and are labeled with inheritance probabilities. The log-likelihood score was shown below each network.

Table 1. References of the four chromosomal taxa included in this study. 2n: diploid chromosome number.

Taxon	2n	Sample locality	References
R. p. chinensis	42	Anhui, China	Zhang 1985
R. p. pearsoni	44	Guizhou, China	Mao et al. 2007
R. yunanensis	46	Sichuan, China	Wu et al. 2006; 2009
R. thailandensis	60	Chiang Mai, Thailand	Harada et al. 1985; Wu et al. 2009

Figure 1

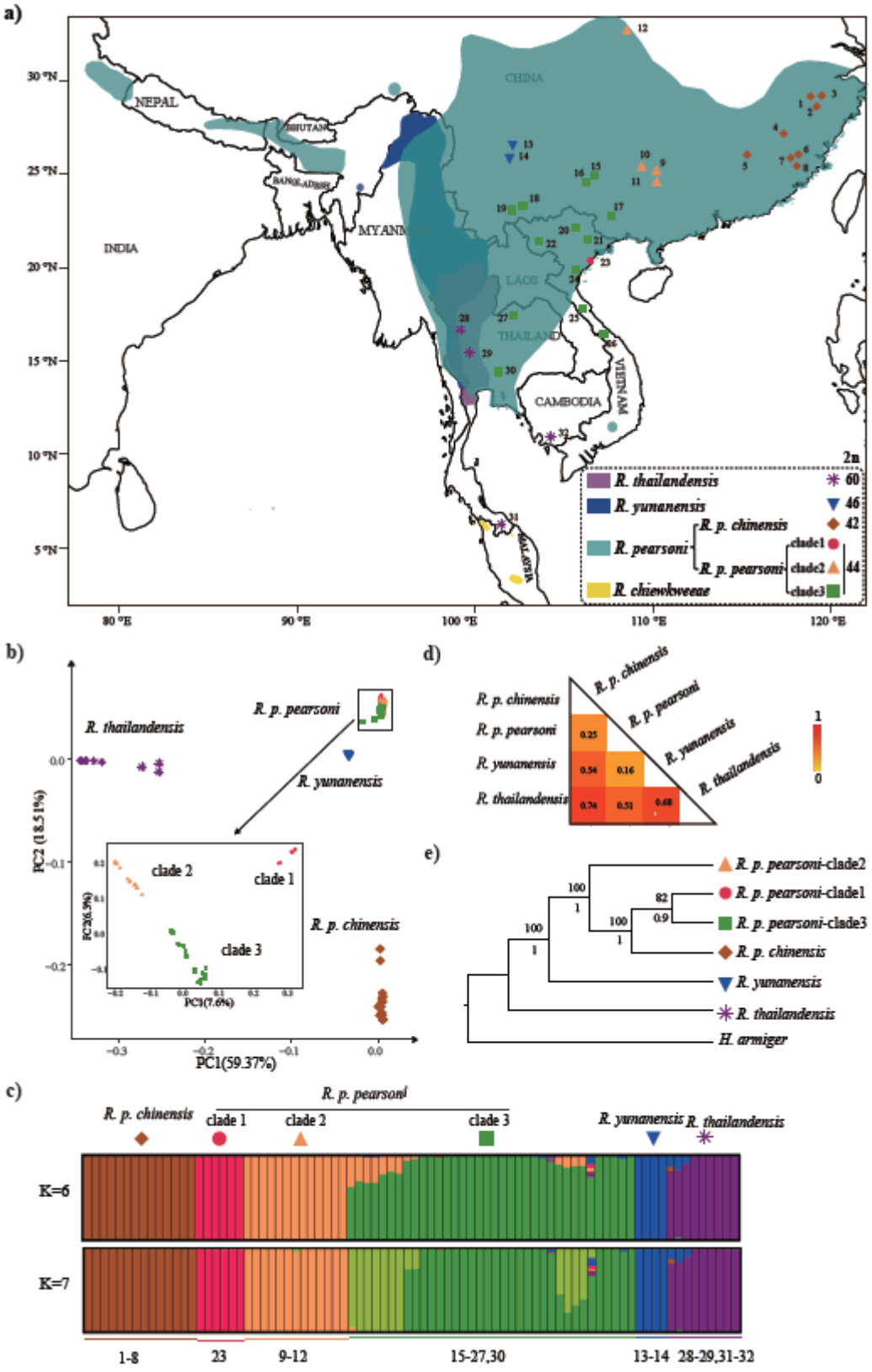
a)
NEPAL
BHUTAN
BANGLADESH
INDIA
MYANMAR
CHINA
LAOS
THAILAND
CAMBODIA
VIETNAM
SRI LANKA
30 °N
25 °N
20 °N
15 °N
10 °N
5 °N
80 °E
90 °E
100 °E
110 °E
120 °E
2n
R. thailandensis
R. yunanensis
R. pearsoni
R. p. chinensis
R. p. pearsoni
clade1
clade2
clade3
R. chiewkweeae
60
46
42
44
b)
R. thailandensis
R. p. pearsoni
R. yunanensis
R. p. chinensis
clade 1
clade 2
clade 3
PC2 (18.51%)
PC1(59.37%)
PC3(6.9%)
PC1(7.6%)
d)
R. p. chinensis
R. p. pearsoni
R. yunanensis
R. thailandensis
0.25
0.54
0.16
0.74
0.51
0.68
1
0
e)
R. p. pearsoni-clade2
R. p. pearsoni-clade1
R. p. pearsoni-clade3
R. p. chinensis
R. yunanensis
R. thailandensis
H. armiger
100
1
82
0.9
c)
R. p. chinensis
R. p. pearsoni
clade 1
clade 2
clade 3
R. yunanensis
R. thailandensis
K=6
K=7
1-8
23
9-12
15-27,30
13-14
28-29,31-32

Figure 2.

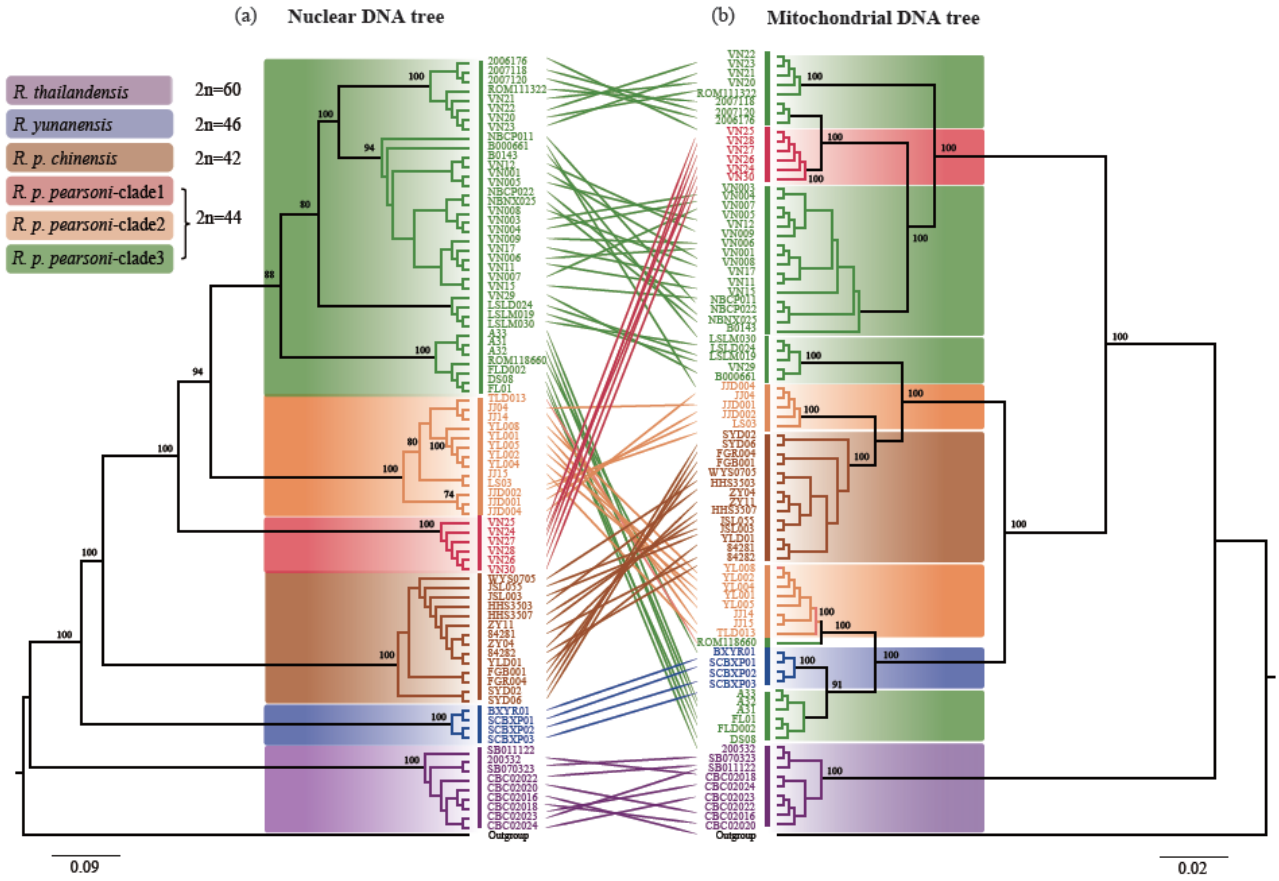
(a) Nuclear DNA tree
(b) Mitochondrial DNA tree
R. thailandensis
R. yunanensis
R. p. chinensis
R. p. pearsoni-clade1
R. p. pearsoni-clade2
R. p. pearsoni-clade3
2n=60
2n=46
2n=42
2n=44
Outgroup
0.09
0.02

Figure 3.

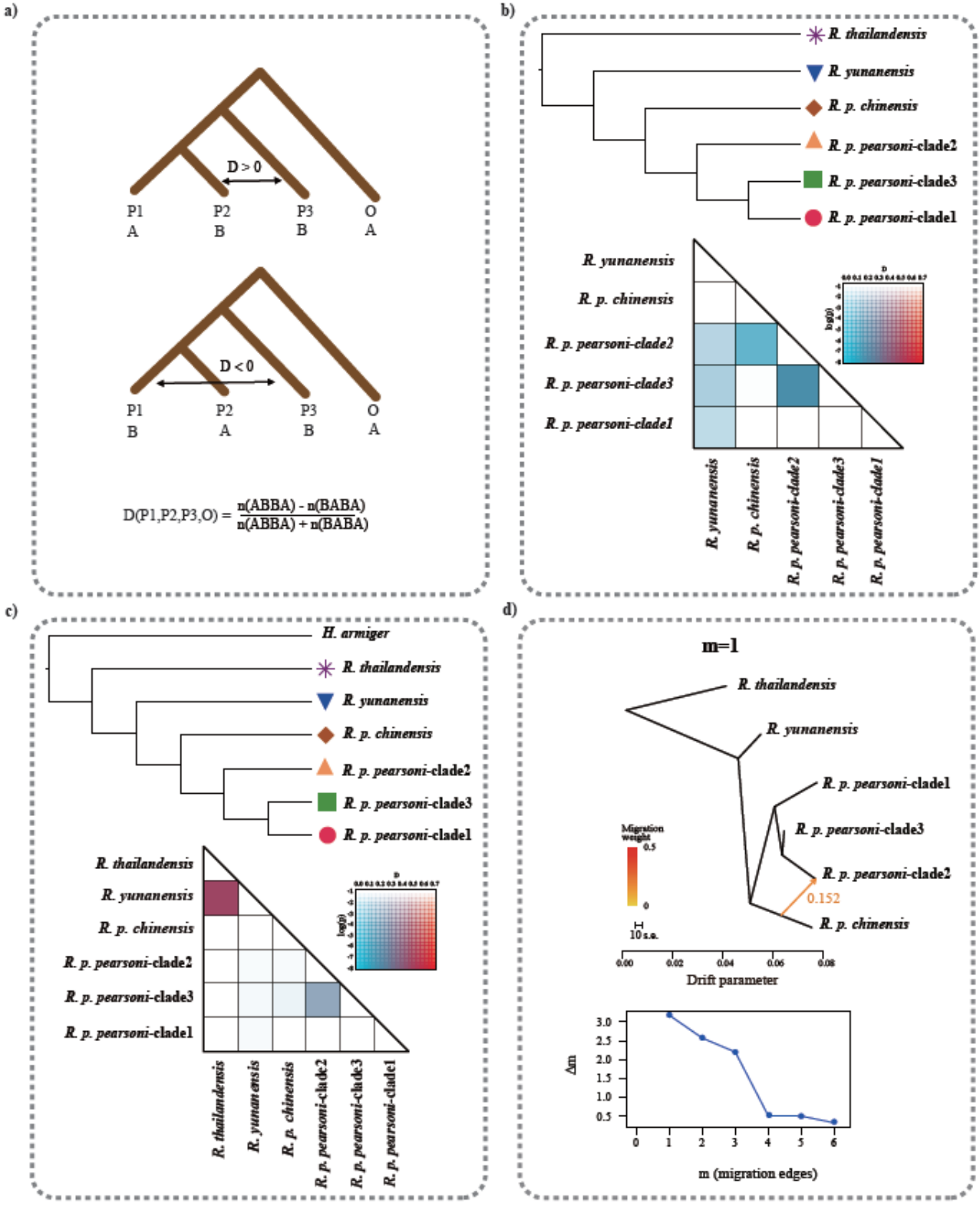
a)
D > 0
P1 A
P2 B
P3 B
O A
D < 0
P1 B
P2 A
P3 B
O A
D(P1,P2,P3,O) = n(ABBA) - n(BABA) / n(ABBA) + n(BABA)
b)
R. thailandensis
R. yunanensis
R. p. chinensis
R. p. pearsoni-clade2
R. p. pearsoni-clade3
R. p. pearsoni-clade1
c)
H. armiger
R. thailandensis
R. yunanensis
R. p. chinensis
R. p. pearsoni-clade2
R. p. pearsoni-clade3
R. p. pearsoni-clade1
d)
m=1
R. thailandensis
R. yunanensis
R. p. pearsoni-clade1
R. p. pearsoni-clade3
R. p. pearsoni-clade2
0.152
R. p. chinensis
Migration weight
0.5
0
10 s.e.
0.00
0.02
0.04
0.06
0.08
Drift parameter
Δm
3.0
2.5
2.0
1.5
1.0
0.5
0
1
2
3
4
5
6
m (migration edges)

Figure 4.

a)

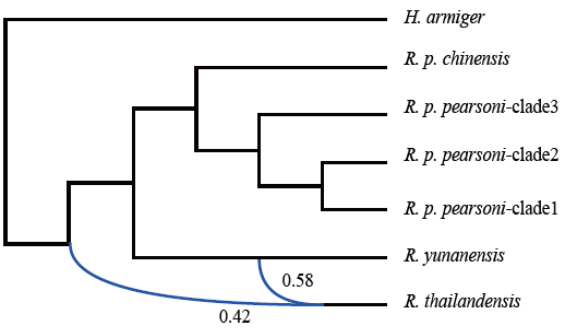

1 reticulations

log(likelihood)= -35665834

b)

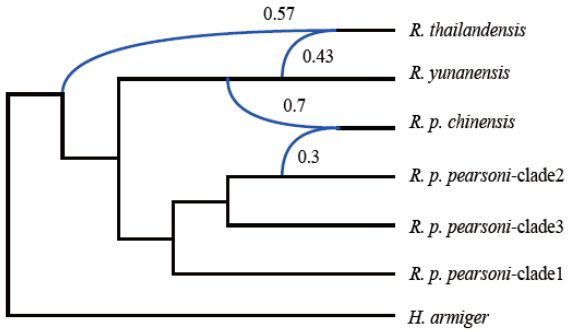

2 reticulations

log(likelihood)= -35626226